Journal of Applied Electrochemistry **32**: 19–23, 2002.

Molten $V_2O_5/Cs_{0.9}K_{0.9}Na_{0.2}S_2O_7$ and $V_2O_5/K_2S_2O_7$ catalysts as electrolytes in an electrocatalytic membrane separation device for SO_2 removal

S.B. RASMUSSEN[1], K.M. ERIKSEN[1], R. FEHRMANN[1]* and J. WINNICK[2]
[1]*ICAT (Interdisciplinary Research Center for Catalysis) & Department of Chemistry, Technical University of Denmark, DK 2800 Lyngby, Denmark*
[2]*School of Chemical Engineering, Georgia Institute of Technology, GA 30332, USA*
*(*author for correspondence, e-mail: rf@kemi.dtu.dk)*

Received 30 April 2001; accepted in revised form 2 October 2001

Key words: catalysis, electrochemical SO_2 removal, $K_2S_2O_7$, membrane separation, molten salt, V_2O_5

Abstract

Bench scale fuel cell tests have been carried out on the SO_2 oxidation catalyst systems $V_2O_5/M_2S_2O_7$ (M = alkali) used as electrolytes in a standard molten carbonate fuel cell (MCFC) fuel cell setup for removal of SO_2 from power plant flue gases. Porous $Li_xNi_{(1-x)}O$ electrodes were used both as anode and cathode. The cleaning cell removes SO_2 when a potential is applied across the membrane, potentially providing cheap and ecological viable means for regeneration of SO_2 from off-gases into high quality H_2SO_4. Results show that successful removal of up to 80% SO_2 at 450 °C can be achieved at approximately 5 mA cm^{-2}. However, the data obtained during the experiments explain the current limitations of the process, especially in terms of electrolyte wetting capability and acid/base chemistry of the electrolyte.

1. Introduction

Emission of sulfur dioxide (SO_2) into the atmosphere is one of the great sources of acid deposition. Coal-burning utilities, Claus plants, ore smelters, sulfuric acid plants and petroleum refineries are the major SO_2 emitters.

Removal processes have been developed, usually based on modified sulfuric acid catalysts which oxidize SO_2 to SO_3; the SO_3 is absorbed by wet film condensers and H_2SO_4 of commercial quality is produced [1]. Unfortunately these processes are generally not economic today, due to high process costs and the low market value of sulfuric acid.

A selective membrane process with only electricity as reagent could remove sulfur species from the flue gas in a much more sustainable and economic process than those currently available.

The membrane consists of an entrained, catalytically active molten salt in an inert porous ceramic matrix, providing a separator for a set of electrodes (Figure 1 shows the setup). This setup provides a pathway for SO_2 and O_2 to react with two electrons and form SO_4^{2-} on one side, followed by transport to the other side where the reaction is reversed and the sulfur species is decomposed and released as SO_3 into a sweep gas. Transport is driven by a potential gradient rather than a pressure gradient. This should enable a high selectivity and efficiency. The capillary forces of the ceramic must be controlled such that the separator matrix should stay filled, while the electrodes must have a more open structure so that the gas/liquid/solid interfacial areas are kept optimal. The molten salt membrane is similar in its construction to the commercial molten carbonate fuel cell (MCFC); this relatively inexpensive, available technology can be modified to suit the purpose of this process.

2. Process chemistry

In 1983 Townley and Winnick [2] introduced the concept using the (Li, Na, K)$_2SO_4$ molten sulfate eutectic at 550 °C with $Li_2O \cdot 9Cr_2O_3$ electrodes. They stated that the two half-reactions would be:

$$\text{Cathode:}\quad SO_2 + O_2 + 2\,e^- \rightarrow SO_4^{2-} \tag{1}$$

$$\text{Anode:}\quad SO_4^{2-} \rightarrow SO_3 + \frac{1}{2}\,O_2 + 2\,e^- \tag{2}$$

This was in accord with classical work on the Li_2SO_4–Na_2SO_4–K_2SO_4-system [3], but supposedly should apply in general to all cases of electrolysis of oxy-anion melts.

Due to the unwanted high temperature of operation the electrolyte was later modified to contain only K^+ as cation, which leads to a significantly lower liquidus point of the salt due to formation of $K_2S_2O_7$ (m.p. 419 °C [4]). According to Franke and Winnick [5] this changed the overall cathode reaction to

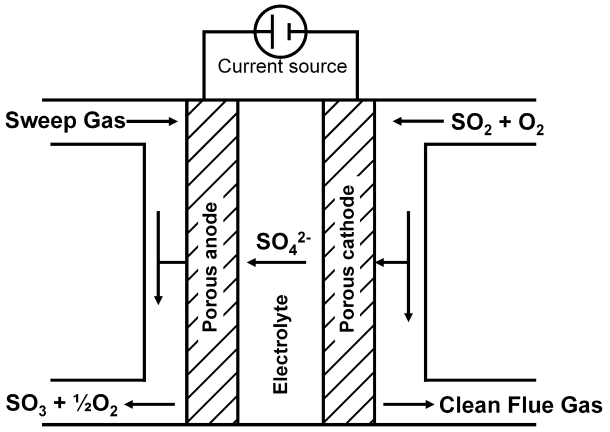

Fig. 1. Principal drawing of membrane process for removal of SO_2 from power plant flue gasses.

$$2\ S_2O_7^{2-} + 2\ e^- \rightleftarrows 3\ SO_4^{2-} + SO_2 \tag{3}$$

in agreement with Durand et al. [6] and later Bjerrum et al. [7].

Since SO_2 was generated in the membrane during processing, 1 wt.% V_2O_5 was added to the $K_2S_2O_7$ based melt for reoxidation of SO_2 in the electrolyte . The process ran at temperatures below 400 °C, so in order to prevent solidification of the melt it was also necessary to add an external pre-oxidation device in the form of a Pt/silica or $V_2O_5/M_2S_2O_7$ (M = K, Na) based catalyst for oxidation of SO_2 from the flue gas. The reactions could then be written:

Flue gas:

$$SO_2 + \frac{1}{2}\ O_2 \xrightarrow{\text{catalyst}} SO_3 \tag{4}$$

followed by a Lux-Flood [8] acid/base reaction:

$$SO_3 + SO_4^{2-} \rightleftarrows S_2O_7^{2-} \tag{5}$$

where SO_4^{2-} is produced at the cathode:

$$\text{Cathode:}\quad 2\ S_2O_7^{2-} + 2\ e^- \rightleftarrows 3\ SO_4^{2-} + SO_2 \tag{6}$$

The SO_2 formed is then re-oxidized catalytically by the electrolyte:

$$\text{Reoxidation:}\quad SO_2 + \frac{1}{2}\ O_2 \rightleftarrows SO_3 \tag{7}$$

followed by the fixation process:

$$\text{Acid/base:}\quad SO_3 + SO_4^{2-} \rightleftarrows S_2O_7^{2-} \tag{8}$$

and finally SO_3 is released at the anode:

$$\text{Anode:}\quad SO_4^{2-} \rightleftarrows SO_3 + 2\ e^- + \frac{1}{2}\ O_2 \tag{9}$$

yielding the same overall reaction across the cell as found for Equations (1) and (2), i.e. $SO_2 + \frac{1}{2}O_2 \rightarrow SO_3$.

However, this electrolyte system has similarities with the industrial supported-liquid-phase catalyst for SO_2 oxidation. The chemistry for that system has been studied extensively for decades and is very complicated. Adding V_2O_5 introduces some new redox reactions to the electrochemical system. Possible electrode reactions may include:

$$S_2O_7^{2-} + V^{V}O_2(SO_4)_2^{3-} + e^- \rightleftarrows V^{IV}O(SO_4)_2^{2-} + 2\ SO_4^{2-} \tag{10}$$

$$S_2O_7^{2-} + (V^{V}O)_2O(SO_4)_4^{4-} + 2\ e^- \rightleftarrows 2\ V^{IV}O(SO_4)_2^{2-} + 2\ SO_4^{2-} \tag{11}$$

where Equation (11) could either occur via a stepwise reduction path where each vanadium atom, separated by a bridging oxygen in the dimer [9], is reduced separately by a one-electron process [7] or by a two-electron process [5]. $V^{IV}O(SO_4)_2^{2-}$ is reoxidized by SO_3 to a V(V) compound and SO_2 which is reoxidized catalytically [10]. Reverse reactions are likely to go on at the anode side and the overall result is again transport of sulfur oxides through the membrane.

$(VO)_2O(SO_4)_4^{4-}$ is regarded as the catalytic active species for SO_2 oxidation [10–12] and precipitation of V(IV) compounds are known to deactivate the catalyst between 380 and 430 °C depending on the chemical environment. Such compounds have been identified as: $Na_8(VO)_2(SO_4)_6$ [13], $Na_2VO(SO_4)_2$ [14], $K_4(VO)_3(SO_4)_5$ [15], $Rb_2(VO)_2(SO_4)_3$, $Cs_2(VO)_2(SO_4)_3$ [16] and $VOSO_4$ [17, 18].

Schmidt et al. [19] instead investigated K_2SO_4–V_2O_5 mixtures above 500 °C but found that, though the vanadium complexes were partly present as vanadates, V(IV) crystalline compounds were still formed at operation conditions. This was probably caused by the high V_2O_5 content (40 mol%) in the molten phase.

Here we propose an electrolyte melt that makes use of the catalytic activity of the melt by using alkali cations (Na^+, K^+ and Cs^+) forming stable pyrosulfates at temperatures in the range 450–500 °C. This would benefit the catalytic oxidation by minimizing deactivation due to solidification as well as enhancing the solubility limit [11] of SO_4^{2-} in $S_2O_7^{2-}$.

3. Experimental

As electrodes semiconducting $Li_xNi_{(1-x)}O$ was used since this type is stable and conductive with low polarization during process conditions [20]. Several ceramics, for use as the matrix, are known to be inert and stable in this electrolyte. Si_3N_4, SiC and yttria-stabilized zirconia (YSZ – from Zircar 65% porosity) can be used with good results. We chose commercially available mats of YSZ. The electrodes were made of 1.25-mm thick National Standard Fibrex mats of high purity Ni fiber with 86% porosity. Electrodes were cut to size from the mat, then lithiated by soaking in an

aqueous solution of LiOH for at least 20 min, dried over a flame, then oxidized in air at 575 °C for several hours. The resultant material was jet-black in color. Mixtures of alkali pyrosulfates where prepared [16] by thermal decomposition of the respective alkali peroxodisulfates. $Cs_2S_2O_8$ was synthesized by reacting CsOH with $(NH_4)_2S_2O_8$ (Merck p.a.) according to a method described earlier [21]. $Na_2S_2O_8$ and $K_2S_2O_8$ as well as V_2O_5 were analytical grade from Merck. Two types of electrolytes were used, a $K_2S_2O_7/V_2O_5$ mixture with a molar ratio of 8 and a $(Cs_{0.9}K_{0.9}Na_{0.21})S_2O_7/V_2O_5$ electrolyte with M/V molar ratio of 6.4. These rather high molar ratios (i.e. low vanadium concentrations) were chosen since preliminary measurements [22] of electrolytes with M/V ratios of 4 seemed to deactivate due to V(IV) compound precipitation at low current densities. All handling of chemicals prior to testing was done in a glove box with less than 20 ppm H_2O.

Housings for bench scale testing of removal performance were made from machined 316 stainless steel. The two identical housings had 8 cm^2 circular wells for electrodes and gas channels to provide baffled gas flow to the electrode. The electronically conductive housings also served as current collectors, as seen in Figure 1.

The pieces were assembled with electrodes in the wells and the ceramic matrix sandwiched between the two housings. The top housing had a hole drilled in it for possible use of a reference electrode and could also be used if electrolyte addition was necessary.

The assembled cell was placed in a brick furnace, and the temperature was controlled with a Barber–Coleman Model 122B controller connected to a double-pole solenoid which controlled the temperature within ± 2 °C. A PAR 173 potentiostat/galvanostat was used to control current applied to the cell. Cell potentials were monitored both on the LCD display on the potentiostat/galvanostat and by Simpson 460 multimeters.

Simulated flue gas with the composition 0.3% SO_2, 3% O_2, $\sim N_2$ provided by Matheson was fed to the compartment containing the cathode, while N_2 from Air Products was fed to the anode side as purge gas. Analysis of SO_2 content was performed with a Perkin–Elmer AutoSystem XL gas chromatograph, equipped with a Supelco 60/80 Chromosorb 102 $2 \times 1/8''$ column and a Flame Photometric Detector (FPD) which conveniently only monitored sulfur species, thus eliminating possible separation problems of effluents. SO_3 concentrations were determined by absorbing the effluent in de-ionized water followed by pH measurements, following a procedure developed by Franke and Winnick [5]. Any positive error in reading due to partial absorption of SO_2 in the sample was regarded as insignificant.

4. Results and discussion

The bench scale tests were conducted with similar experimental conditions such that only the variation in electrolyte and temperature would influence the data. Removal data show that $K_2S_2O_7$–V_2O_5 based melts exhibit sufficient catalytic activities at temperatures between 440 and 480 °C. Apparently the catalytic oxidation is improved when the reaction product (SO_3) is removed from the cathodic interface by applying current. This must be due to a low SO_2/SO_3 molar ratio near the interface resulting from a concentration profile of SO_2 from the bulk gas phase to the surface of the electrolyte melt in the cathode pore structure. Using the $M_2S_2O_7$–V_2O_5 type electrolyte enhances the catalytic oxidation, as expected from Ref. [10]. The $K_2S_2O_7$–V_2O_5 melt at 443 °C emits approximately 600 ppm SO_x at 4.0 mA cm^{-2} (see open squares in Figure 2) corresponding to 80% removal of all sulfur oxides. Five hundred ppm of the residual flue gas sulfur oxides are released as SO_2 in the cathode outlet (in the cleansed flue gas) while the other approximately 100 ppm are released from the cathode compartment as SO_3. The $M_2S_2O_7$–V_2O_5 based melts, though good for oxidation, are less efficient compared to $K_2S_2O_7$–V_2O_5 at removing SO_3 across the membrane cell.

A sudden collapse of the process occurred during all tests. This can be seen in Figures 2–5 as a significant change in the gas composition of the outlet when a threshold value is reached. With the $V_2O_5/Cs_{0.9}K_{0.9}Na_{0.2}S_2O_7$ based melt this threshold value is 2.0 mA cm^{-2} both at 443 °C (Figure 4) and at 475 °C (Figure 5). For the $V_2O_5/K_2S_2O_7$ melt it occurs at 4.0 mA cm^{-2} at 443 °C (Figure 2) and at 3.0 mA cm^{-2} at 475 °C (Figure 3). This phenomena was expected to occur due to insufficient catalytic oxidation of the incoming SO_2, but since SO_3 was present in the cathode outlet gas stream in all cases and in major amounts with the $V_2O_5/Cs_{0.9}K_{0.9}Na_{0.2}S_2O_7$ based melt, this is not likely to be the explanation with these systems at these temperatures.

Since insufficient catalysis is not limiting the process, it would be beneficial to examine the polarization

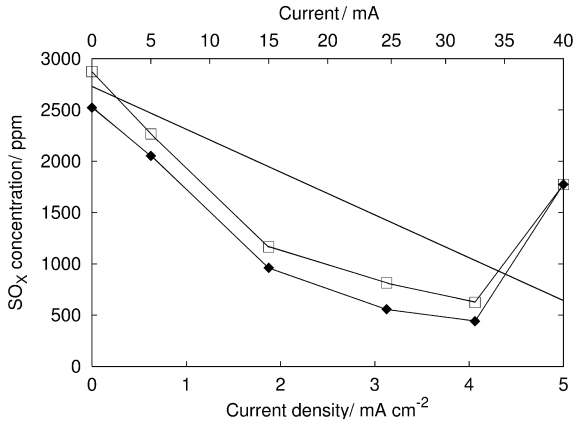

Fig. 2. Cathodic performance data of a $K_2S_2O_7$–V_2O_5 melt with a $K_2S_2O_7/V_2O_5$ molar ratio of 8 at 443 °C. Gas composition: 0.28% SO_2, 8% O_2, 10% H_2O, $\sim N_2$; Volumetric flow rate 125 ml min^{-1}; (□): Total sulfur (SO_x) emission; and (♦): SO_2 emission in flue gas after exposure to cell; The solid line represents expected SO_x transfer with a 2F per mole Faradaic reaction pathway.

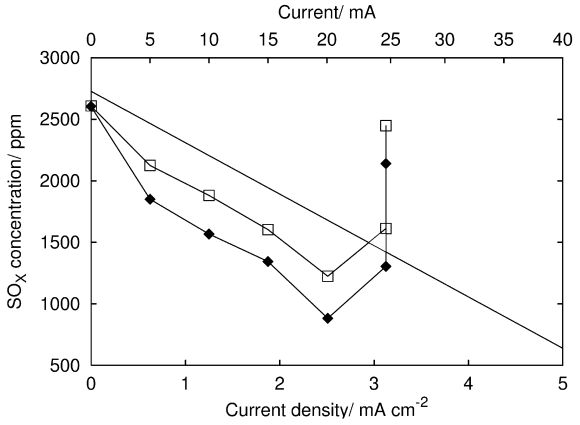

Fig. 3. The same as mentioned in Figure 2 at 475 °C (with similar gas composition).

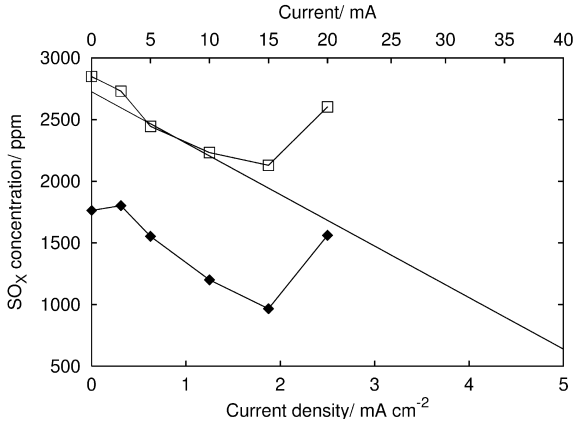

Fig. 4. Cathodic performance data of a $M_2S_2O_7$–V_2O_5 melt with a $M_2S_2O_7/V_2O_5$ molar ratio of 6.4 (M = 10% Na, 45% K, 45% Cs). Temperature was 443 °C; Gas composition: 0.28% SO_2, 8% O_2, 10% H_2O, ~N_2; Volumetric flow rate 125 ml min^{-1}; (□): Total sulfur (SO_x) emission; and (◆): SO_2 emission in flue gas after exposure to cell; The solid line represents expected SO_x transfer with a 2F per mole Faradaic reaction pathway.

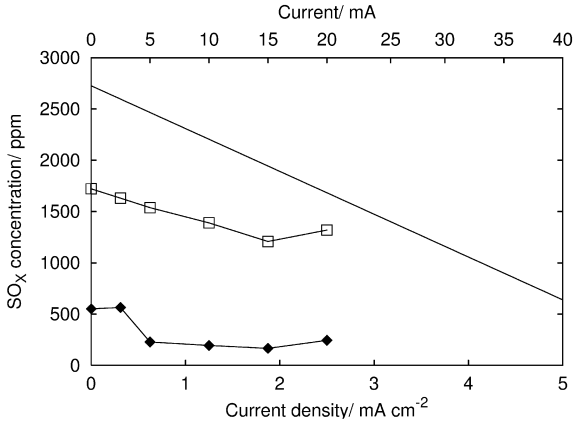

Fig. 5. Cathodic performance data of a $M_2S_2O_7$–V_2O_5 melt with a $M_2S_2O_7/V_2O_5$ molar ratio of 6.4 (M = 10% Na, 45% K, 45% Cs). Temperature was 475 °C. The conditions are the same as mentioned in Figure 4.

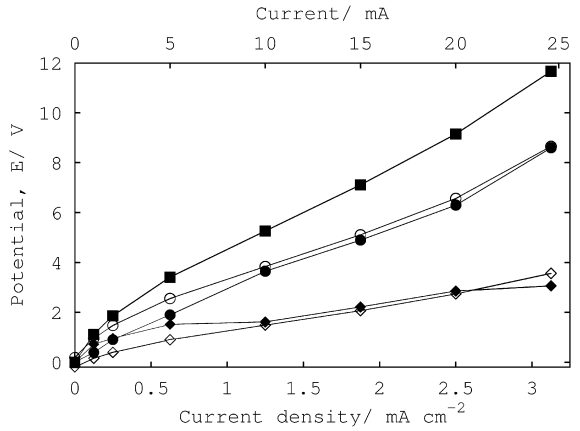

Fig. 6. Polarization performance data of a $M_2S_2O_7$–V_2O_5 melt with a $M_2S_2O_7/V_2O_5$ molar ratio of 6.4 (M = 10% Na, 45% K, 45% Cs) at 443 °C. Gas composition: 0.28% SO_2, 8% O_2, 10% H_2O, ~N_2; Volumetric flow rate 125 ml min^{-1}; Reference was a gold wire in contact with electrolyte purged by same simulated flue gas; (■): Polarization across entire membrane cell; (○): Anode-reference point polarization; (●): Ohmic resistance across entire membrane cell; (◆): Polarization across entire membrane cell after subtraction of Ohmic contribution; (◇): Cathode-reference point polarization.

performance during these bench scale tests. The total polarization and the ohmic contribution across the membrane were monitored during all tests. The corrected polarization increased in all cases with applied current and reach 1.5–2.0 V at 2.0 mA cm^{-2} (Figure 6). This contribution is mainly due to mass transfer limitations. However, much more significant is the increase in ohmic resistance with increasing current compared to the expected Ohmic law resistance. This could be caused by the mentioned deactivation process, where crystalline, non-conductive V(IV) and/or V(III) compounds precipitate at the cathode interface. This causes poor conductance across the cell and also contributes to loss of cathode interface surface area; this partly explains the high ohmic-corrected polarization. However, since oxidation catalysis appears to continue sufficiently and precipitation seems to occur only below 440 °C [16] it is unlikely that the pores of the cathode are filled with these species. Another explanation is precipitation of electrolyte at the anode interface, but since the V(V)/V(IV) ratio should be high here due to the positively charged anode, and since the SO_3 activity should be high due to the decomposition reaction in Equation (2), it is unlikely that precipitation of V(IV) compounds occurs.

In addition V(V) compounds known in the V_2O_5–$M_2S_2O_7$–SO_3 systems have melting points lower than 420 °C [21, 23–26]. The polarization data shown in Figure 6 were obtained with a $V_2O_5/Cs_{0.9}K_{0.9}Na_{0.2}S_2O_7$ (M/V = 8) melt at 475 °C, but the general trends are expected to apply to all systems since the polarization data for all tests showed similar behavior. Using the reference point to separate contributions from the anode- and cathode sides it became obvious that conductivity was decreasing at the anode interface. The corrected polarization contribution appeared at the

cathode side as expected, since here a complicated reaction scheme with gas–electrolyte–electrode interfaces is expected to follow Equations 4–11.

This behavior can be explained by considering mobilities of the ions in the electrolyte. The cations are Na^+, K^+ and Cs^+, while the anions are SO_4^{2-}, $S_2O_7^{2-}$, $(VO)_2O(SO_4)_4^{4-}$ and $VO_2(SO_4)_2^{3-}$. The cations have significantly higher mobilities than their counter-ions. This could lead to general movement of the melt into the cathode pores. Since cations are attracted to the negatively charged cathode they migrate in this direction, and since charge neutrality must be upheld, the anions must follow. This results in flooding of the cathode pores and leads to poor contact between the anode and electrolyte, which also was visually observed. The net effect is an increase in ohmic polarization on the anode side, and a corrected polarization increase on the cathode side. The potential must increase in order to maintain the same current. This increases the potential gradient between the anode and the cathode, so that migration towards the cathode is increased. This explains the almost exponential-like increases in ohmic polarization with increase in current (Figure 6).

This will happen when the external forces (due to pore size distribution and capillary forces) are equal for anode and cathode ceramics. A possible solution could be to adjust the pore size of the anode ceramics such that it balances both the capillary forces from the cathode ceramics and the electrical field force described above. Also minimizing the thickness of the separator matrix and the area of charged housing parts in contact with the melt, are of major importance for further development of the process.

Furthermore the release of even minor amounts of SO_3 from power plant off-gases is disastrous for the local environment and must be avoided. This can be minimized by using melts with lower catalytic activity and higher sulfate content which will make the melts more basic, thus enhancing the melt affinity for SO_3. Therefore electrolytes based on Li, Na and K pyrosulfates and V_2O_5 are promising candidates. In long term runs the $M_2SO_4/M_2S_2O_7$ ratio will reach a steady-state solely dependent on alkali (M^+) properties and temperature. At these experimental conditions (setup running for 2–3 days for each test) the melts were too acidic and an appropriate steady-state was not reached, characterized by too effective oxidation and insufficient transport across the cell.

5. Conclusion

An electrical membrane separation device for flue gas removal has been modified such that it runs with integrated catalytic oxidation at reasonable temperatures (~450 °C). A new explanation of process limitation has been determined and explored. It has been found that minimizing flooding of the cathode and poor conductance on the anode side are major factors in improving the process. However, substantial research is required in order to reach sufficient cleaning of the flue gas of around 90% at higher current densities i.e. in the range 20–25 mA cm^{-2}, which is considered economically viable.

Acknowledgement

NATO (Science for Peace Project SFP 971984) has supported this investigation.

References

1. J. Andreasen, J.K. Laursen, O.R. Bendixen and H. Topsøe, *Int. Power Gen.* **15** (1992) 58.
2. D. Townley and J. Winnick, *Electrochim. Acta* **28** (1983) 389.
3. K.E. Johnson and H.A. Laitinen, *J. Electrochem. Soc.* **110** (1960) 314.
4. N.H. Hansen, R. Fehrmann and N.J. Bjerrum, *Inorg. Chem.* **21** (1982) 744.
5. M. Franke and Winnick, *J. Electroanal. Chem.* **238** (1987) 163.
6. A. Durand, G. Picard and J. Vedel, *J. Electroanal. Chem.* **70** (1976) 55.
7. N.J. Bjerrum, I.M. Petrushina and R.W. Berg, *J. Electrochem. Soc.* **142** (1995) 1809.
8. H. Flood and T. Førland, *Acta Chem. Scand.* **1** (1947) 781.
9. K. Nielsen, R. Fehrmann and K.M. Eriksen, *Inorg. Chem.* **32** (1993) 4825.
10. O.B. Lapina, B.S. Bal'zhinimaev, S. Boghosian, K.M. Eriksen and R. Fehrmann, *Catal. Today* **51** (1999) 469.
11. S.B. Rasmussen, K.M. Eriksen and R. Fehrmann, *J. Phys. Chem.* **103** (1999) 11282.
12. S. Boghosian, F. Borup and A. Chrissanthopoulos, *Catal. Lett.* **48** (1997) 145.
13. K. Nielsen, S. Boghosian, R. Fehrmann and R.W. Berg, *Acta Chem. Scand.* **53** (1999) 15.
14. R. Fehrmann, S. Boghosian, G.N. Papatheodorou, K. Nielsen, R.W. Berg and N.J. Bjerrum, *Inorg. Chem.* **29** (1990) 3294.
15. R. Fehrmann, S. Boghosian, G.N. Papatheodorou, K. Nielsen, R.W. Berg and N.J. Bjerrum, *Inorg. Chem.* **28** (1989) 1847.
16. S. Boghosian, R. Fehrmann, N.J. Bjerrum and G.N. Papatheodorou, *J. Catal.* **119** (1989) 121.
17. R. Kierkegaard and J.M. Longo, *Acta Chem. Scand.* **19** (1965) 1906.
18. S. Boghosian, K.M. Eriksen, R. Fehrmann and K. Nielsen, *Acta Chem. Scand.* **49** (1995) 703.
19. D.S. Schmidt, J. Winnick, S. Boghosian and R. Fehrmann, *J. Electrochem. Soc.* **146** (1999) 1060.
20. D.S. Schmidt, D. McHenry and J. Winnick, *J. Electrochem. Soc.* **145** (1998) 892.
21. G.E. Folkmann, G. Hatem, R. Fehrmann, M. Gaune-Escard and N.J. Bjerrum, *Inorg. Chem.* **30** (1991) 4057.
22. S.B. Rasmussen, K.M. Eriksen, R. Fehrmann and J. Winnick, In *Proc. Twelfth International Symposium on Molten Salts*, P.C. Trulove, H.C. De Long, G.R. Stafford and S. Deki (eds.) The Electrochemical Society 99–41, Pennington, NJ, 2000 p. 694.
23. V.N. Krasilnikov, M.P. Glazyrin and A.A. Ivakin, *Zh. Neorg. Khim.* **29** (1984) 94; *Russ. J. Inorg. Chem. (Engl. Transl.)* **29** (1984) 53.
24. G.E. Folkmann, K.M. Eriksen, R. Fehrmann, M. Gaune-Escard, G. Hatem, O.B. Lapina and V. Terskikh, **102** (1998) 24.
25. D.A. Karydis, S. Boghosian and R. Fehrmann, *J. Catal.* **145** (1994) 312.
26. F. Abdoun, G. Hatem, M. Gaune-Escard, K.M. Eriksen and R. Fehrmann, *J. Phys. Chem.* **103** (1999) 3559.